Power System Technology
ISSN:1000-3673

Received: 16-01-2024 Revised: 12-02-2024 Accepted: 07-03-2024

Insitu Hybrid Composites Reinforced with B_4C and Tio_2 in an Al7075 Matrix Formed and It's Mechanical and Wear Properties are Analysed.

Jayanth H[1], Dr. Gangadhar N[2], Dr. K M Purushothama[3]

[1,2] Assistant Professor, Department of Mechanical Engineering, Dr Ambedkar Institute of Technology, Visvesvaraya Technological University, Bangalore-560060, Karnataka, India.
[3]Professor, Department of Mechanical Engineering, Dr Ambedkar Institute of Technology, Visvesvaraya Technological University, Bangalore-560060, Karnataka, India.
Corresponding Author: jayanth.me@drait.edu.in

Abstract-

Hybrid metal matrix composites (MMCs) have growing application of in structural and reliability critical applications and has replacements of ceramics due to their first-class wettability and inherent ductility and toughness. This research is determined on the influence of dealing out on hybrid alumunium composite reinforced right through Al, B4C and Tio_2 reactions. In order to examine the outcome of Al-Ti based intermetallic compounds on the properties in situ Al_3Ti were likely to form over and above TiB and TiC. . The in situ composite that had a B_4C and Tio_2 content of 6wt% of B4C exhibited considerably high strength (20.94kN) and elastic modulus of (169.82N/mm^2).These insitu composites can be accepted to have excellent mechanical strain tolerance. Hardness value was calculated using a Vickers micro hardness tester. It is observed that the 6wt% B4C of reinforcement had highest hardness number (91.90VHN).SEM micrograph observations indicate that the reinforcement was homogeneously distributed in hybrid aluminium metal matrix (HAMC) in addition to Morphological characterization plus wear behaviour of aluminium hybrid composites were investigated, amounts of B_4C (2, 4, and 6wt %) were added to. The morphological characterization of all synthesized composites was performing using X-ray diffractometer (XRD), Scanning Electron Microscope (SEM), Energy Dispersive Spectrum (EDS) and Elemental Maps. The wear resistance of aluminium hybrid composite (HAMC) reinforced with 6 wt% B_4C particles was highest amongst all the synthesized composites.

Keywords: Hybrid, Insitu, Al_3Ti, composite, TiB_2, TiC, Tio_2, Al-B_4C, Al_2O_3

Power System Technology
ISSN:1000-3673

Received: 16-01-2024 Revised: 12-02-2024 Accepted: 07-03-2024

1. Introduction

A material system with the work of a suitable and smart combination of two or more constituent can be term as composite [1]. The constituent in a composite creation should have an interface in an attempt to be different in both the type and chemical composition that allow for a separation. Composite constituent are insoluble in each other as compare to pure aluminium (Al) and its alloys [2-3]. Owing to this, AMCs are the most extensively investigated metal matrix composites (MMC) and a wide variety of reinforcements in particulate form such as aluminium oxide (Al2O3), boron carbide (B4C), silicon carbide (SiC), titanium carbide (TiC), zirconium oxide (ZrO2), titanium diboride (TiB2), carbon nanotubes (CNTs) and grapheme nanoplatelets (GNPs) have been used in aluminium(Al) to manufacture AMCs [4-5-6]. In addition to using a single reinforcement in AMCs, the scheme of incorporating at least two reinforcements provides an opportunity to modify the properties of composites called hybrid AMCs. Hybrid MMCs: Hybrid MMCs basically hold additional different somewhat reinforcements in addition to individual such as combination of atom and hair a combination of fibre and particle or a combination of hard and cushioned reinforcements [7-8-9]. Aluminium is a vital material for aerospace, transportation, and structural machinery owing to its high strength-to-weight ratio and low specific weight. Aluminium has a sole behaviour of maintaining its toughness down to very low temperatures; nothing like carbon steels would otherwise suffer embrittlement [10-11-12]. On the other hand low hardness (25–35 HV) and low wear resistance are severe apprehension for its long-lasting use in much industrial application. Particle-reinforced MMCs: contain equi-axed ceramic reinforcements, mainly oxides (e.g. alumina, Al_2O_3), carbides (e.g. silicon carbide, SiC) or borides (e.g. titanium bromide, TiB2), with an aspect ratio a smaller amount of five and present in volume fraction not more than 30% [15-16-17]. They can be shaped by blending metal and followed by solid-state sintering or by liquid-metal techniques such as stir casting, squeeze infiltration and in situ processes [18-19-20]. Particulate aluminium matrix composites (AMCs) demonstrate high tensile and compressive strength and better tribological properties than conservative materials. The adding's of hard particles in aluminium forge composite connect the extreme hardness and wear fighting of particulates accompanying depressed mass and ductility of mold happening in good spatial stability of the material [21-22-23]. Particle reinforced composites are better ductility than the whisker or fiber reinforced composites therefore, are preferable over other composites because of their low cost-benefit, excellent heat, and wear-anti properties [24-25]. The reinforcements are established into an alloy cast to reinforce the mechanical and material possessions toact a fundamental aspect but also change the tangible features such as thermal generated power or fighting to wear [26-27]. Hybrid composite accompanying synthetic potteries and environmental pollutant by output start to be acceptable for state-of-the-art uses in automobiles, aerospace, and structural requests on account of their inconsequential low cost, and extreme substance and have the approachability to tailor the properties as per necessities

Power System Technology
ISSN:1000-3673
Received: 16-01-2024 Revised: 12-02-2024 Accepted: 07-03-2024

by selecting acceptable reinforcements [28-29].Due to this approachability and the perfect blend of customizable triboloigical and mechanical possessions, extreme substance weight percentage , and material health, HAMCs are advanced matters containing aluminium alloys oppose unending an discontinuous support types of fabrics exhibit superior properties a fore mentioned the same disintegration and temperature opposition , extreme particular inflexibility and high young's modulus [30-31]. HAMCs composites of aluminium, boron carbide and titanium group of chemical elements offer the superior merger of high severity in a incidental structure [32-33].wear is an apparent case of material replacement that happens in the interface joining two surface and influences the dependability and durability of each vehicle .Consequently wear and substance to weight percentage are critical features of matters needed to develop the efficiency of machine [34-35]

2. Materials and Methods

Table 2.1 insitu hybrid AMCs are Fabricated

insitu hybrid composite	Starting material	Additives and alloying elements	Insitu phase
Al-(TiB_2+W)	Al-B_4C	TiO_2, Ti	W:Tic, Al_2O_3

In Al-B_4C-TiO_2 system the reaction path for the synthesis of the composites depends basically on the Al content.

$$14\mathrm{Tio_2} + \mathrm{B_4C} \rightarrow 4\mathrm{TiBo_3} + 5\mathrm{Ti_2o_3} + \mathrm{Co}$$
$$\mathrm{TiBo_3} + 4\mathrm{B_4C} \rightarrow \mathrm{TiB_2} + 11\mathrm{Bo} + 4\mathrm{Co}$$
$$15\mathrm{AL} + 3\mathrm{Tio_2} \rightarrow 2\mathrm{Al_2o_3} + 3\mathrm{Al_3Ti}$$
$$3\mathrm{Al_3Ti} + \mathrm{B_4C} \rightarrow \mathrm{Tic} + 2\mathrm{TiB_2} + 9\mathrm{Al}$$

A eutectic –type agglomeration structure is obtained, while the insitu particles in isolation spread at higher Al content minor the particle size, during the combustion synthesis Al-B_4C-TiO_2 systems, the reaction kinetics is diffusion controlled. The combustion temperature and size of the insitu formed particles decrease with increasing Al content in systems. The ignition delay time is first reduced and significantly raised with increasing the Al content a reduction in B_4C Particle size facilitates the ignition and self sustain combustion reaction. Al_3Ti phase is established to degrade mechanical properties of the composites Al_3Ti formation can be suppressed by increasing the reaction time and temperature and controlling the proportions [8-12-18].

Power System Technology
ISSN:1000-3673
Received: 16-01-2024 Revised: 12-02-2024 Accepted: 07-03-2024

Table 2.2 Characteristics of Starting material

Starting material	Chemical composition
Al7075	Zn-5.6, Mg-2.5,Cu-1.5,Mn-0.04,Fe-0.3,Si-0.08,Ti-0.1,Cr-0.1
B_4C	Impurities include < 0.8% Fe and < 0.3%B_2O_3
TiO_2	Impurities of < 0.03% ZrO_2 and 0.01% CaO

Table 2.3 Properties of Al7075, Titanium Dioxide and Boron Carbide

Properties	Density g/cm^3	Melting point, ^{o}C	Young's Modulus GPa	Crystal Structure
Al7075	2.81	635	71.7	Hexagonal
B_4C	2.52	2445	450-470	Rhombohedra
TiO_2	3.97	2103	230	Tetragonal

3. Density Calculation:

3.1 Theoretical Density-

$\rho = \frac{n}{V_{Cell}} \frac{A_w}{N_A}$--------eq-3.1 (Appendix-1)

ρ = Theoretical density, n= effective number of atoms per unit cell, A_w= Atomic weight, V_{Cell} = Volume of unit cell, N_A =Avogadro's number (6.022 x 10^{23} atoms/mol),Single cubic (SC) -n=1, Body Centred Cubic (BCC)-n=2, Face centred cubic (FCC) -n=4, Hexagonal Closed packed (HCP)-n=6, Diamond cubic (DC)-n=8, for cubic cell (i.e. SC, BCC, FCC and DC), V_{cell} = a^3, for Tetragonal cell, V_{cell}= a^2*c, for Hexagonal cell (HCP), V_{cell}= (6*sqrt of ¾)* a^2*c, Edge length (a) =412 pm (parts per million)= 412x 10^{-10} cm, Number of atoms (n) = 1,Molecular weight = 168.5 g/mol, Atomic Weight = 63.55 g/mol (1amu=1g/mol),Atomic radius= R=0.128nm (1nm=10^{-7} cm),For FCC a =4$\frac{R}{\sqrt{2}}$,V_c= 4.75 x 10^{-23} cm^3 ,a = 2 R,HCP a distance = 2r,C distance = 4 Sqrt 2/3 r, HCP= 6, Area of base = sqrt ¾ a^2 ,(Hexagonal, made up of equilateral triangle), H be the height of hexagon, h/a =sqrt 8/3 for HCP, volume of HCP = $V = 24\sqrt{2}\, r^3$.

3.2 Experimental Density-

In simple form, the Archimedes law states that the buoyant force on an object is equal to the weight of the fluid displaced by the object written as: F_b= ρ x g x v,Where F_b is the buoyant

Power System Technology
ISSN:1000-3673
Received: 16-01-2024 Revised: 12-02-2024 Accepted: 07-03-2024

force, ρ be the density of the fluid, V is the submerged volume by $\boldsymbol{V = \pi r^2 h}$, and g is the acceleration due to gravity. Density (ρ) is defined as mass (M) by volume (V), mass of the displaced liquid, weight of the displaced liquid can be calculated as follows: weight (w) =Mass (M) x Acceleration due to gravity (ρvg) also known as Thrust force.

Table 3.2 HAMC-validation of Theoretical Density and Experimental Density

HAMC ((Al7075 + B_4C+ Tio_2)	Theoretical Density g/cm^3	Experimental Density g/cm^3
0% wt composition	2.6713	2.4623
2% wt composition	2.7213	2.5743
4% wt composition	2.7713	2.6793
6% wt composition	2.8213	2.4183

4. Tensile test-

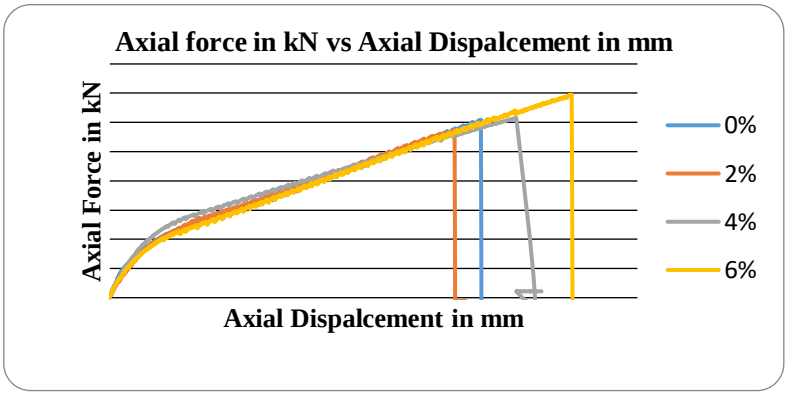

Figure 4.1 Axial forces vs. Axial displacement in mm

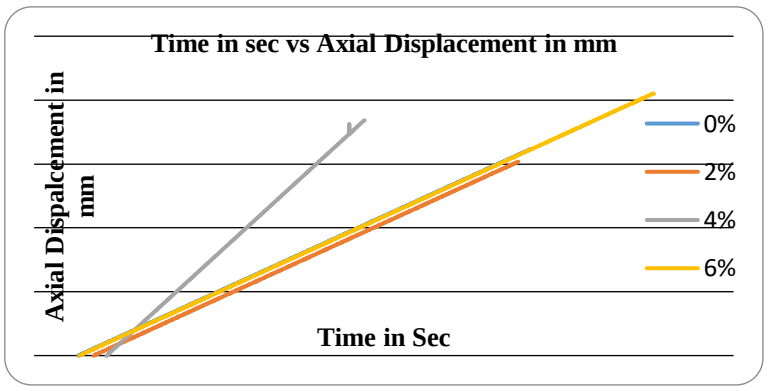

Figure 4.2 Time in sec vs. Axial displacement in mm

Power System Technology
ISSN:1000-3673
Received: 16-01-2024 Revised: 12-02-2024 Accepted: 07-03-2024

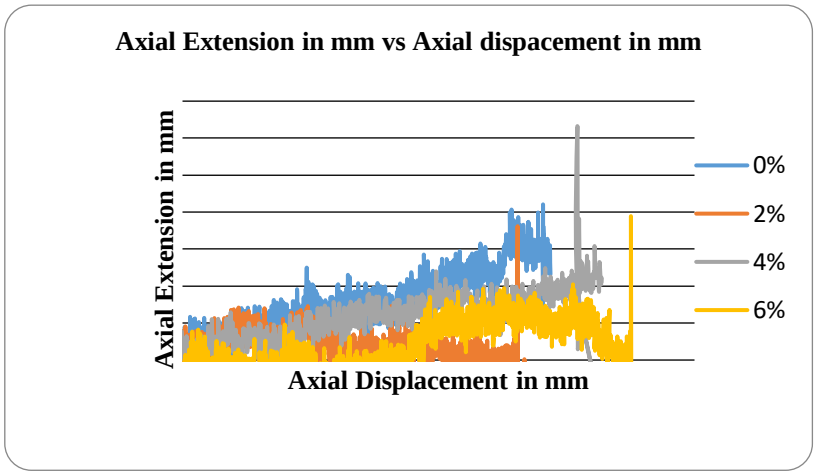

Figure 4.3 Axial Extension in mm vs. Axial displacement in mm

Mechanical properties of composites were assessed by means of universal testing machine MTS-809 electro-hydraulic servo testing machine, according to E8 ASTM standard with a maximum load of 250 KN and a data acquisition rate of 8 points/s. Strain was measured by extensometer with gauge distance of 10 mm, and the extensometer model is Mechanical Testing and Simulation Systems Corporation MTS647. A graph of axial force in KN vs axial displacement in mm, time vs axial displacement and axial extension vs axial displacement is plotted with diiffrent weight percentage of 0%wt, 2% wt, 4%wt and 6%wt with insitu reaction (Al7075 + B_4C+ Tio_2) hybrid alumunium composites.

A graph plotted axial force in kN vs axial displacement in mm is within the elsticic limit and holds good for hooke's law from the graph 0.1 to 0.3 displacement the curve is linear within the elastic limit of the composite, composite yeilding process is taken place and from their ductility of the composite has incresased with varying percentage of B_4C and impact energy of maximum 2.4J/mm^2.

0 mm to 2mm the energy aborsobed in that range is 0.2% proof resilence like 0%,2%, 4% and 6% and maximum load of 17.15 kN,18.26 kN,18.72 kN and 20.94 kN with diameter 12.5 mm ultimate stress of the material are 139.71 N/mm^2, 139.83 N/mm^2, 150.34 N/mm^2 and 169.82 N/mm^2 and composite fails at 1.2 mm,1.3mm,1.5mm and 1.65mm fails at this dispalement it clearly evident that ductility of the composite is increasing. With 2 wt% of reinforcement B_4C in hybrid metal matric composite the chemical endothermic insitu rection with alumunium reinforcement are weakened from the rule of mixture.In the displcement range of 0.3mm to 1.1mm from the graph axial force is increasing constantly with axial displcement. A graph plotted axial displcement in mm vs time in sec displcemnet is directlly propotional to time as displcement in the ductile composite varying linearly with time by varying percentage of reinforcemnet in hybrid metal matrix composites(HAMC) among this 6% of B_4C their is

Power System Technology
ISSN:1000-3673
Received: 16-01-2024 Revised: 12-02-2024 Accepted: 07-03-2024

mnaximum displcement with maximum time in seconds.A graph plotted axial displcement vs axial extension with constant ststic application of load in kN the extension of the composite taking place with constant load and extension is measured using an extensometer in millimeter and finally failure at maximum displcement.

5.Compression test-

Compression test was conduted in universal testing machine based on E9 ASTM satandard diameter of the specimen was 25mm and thickness of 30mm and graph of load vs Dispalcement is plotted with diiffrent weight percentage of 0%wt, 2% wt, 4%wt and 6%wt with insitu reaction (Al7075 + B_4C+ Tio_2) hybrid alumunium composites. A graph plotted with load in kN and displcement in mm a static compressive force applied on the material with varying composite of B_4C from the displcement 0 mm to 2mm the energy aborsobed in that range is 0.2% proof resilence with 0%wt, 2% wt, 4%wt and 6%wt with maximim force of 237.3kN, 243.9kN, 263.15kN and 277.22kN amd failure at maximum displscement of 7.1mm, 7mm, 7.4mm and 8.6mm repectivley.it is clesrly evident from the graph that with 2 wt% of reinforcement B_4C in hybrid metal matric composite the chemical endothermic insitu rection with alumunium reinforcement are weakened or less than the 0wt%.

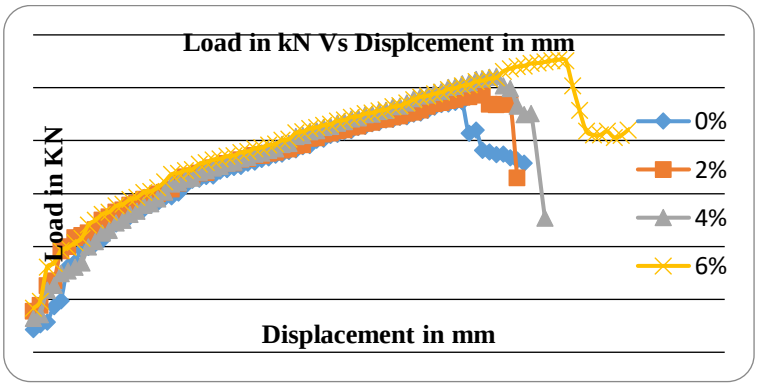

Figure 5.1 Loads in KN vs. Axial Displacement in mm

6. Impact test-

Izod test was performed as per ASTM standard D256 with angle of drop 85^0 degrees and weight of the pendulum is 21.926kg, thickness and width of the specimen is 7mm and 10mm.

Table 6.1 Impact strength of HAMC weight percentage

HAMC	0%	2%		4%	6%
Impact Strength J/mm^2	2.214	2.328		2.457	2.661

Power System Technology
ISSN:1000-3673
Received: 16-01-2024 Revised: 12-02-2024 Accepted: 07-03-2024

7. Wear rate-

Wear rate is ratio of wear amount to sliding distance or time and SI units in m^3/m and wear amount is given by volume loss (m^3)* mass loss(kg) * linear dimension change (m) and experimental test conducted on synthesize composites using pin on disc apparatus according to the standard ASTM-G99. with diiffrent weight percentage of 2% wt, 4%wt and 6%wt with insitu reaction (Al7075 + B_4C+ Tio_2) with abrading length calculated on pin disc where D is the circumference and t is in sec and sliding distance (500,750 and 1000) and at load conditions 2Kg,4Kg and 6Kg. The disc on the wear testing machine was cleaned by solution after each test to avoid entrapment of the remaining particles from the earlier test. The wear test was performed on specimens at a particular value of load and then the calculation of wear was done. It is observed from the graph that for the loading conditions of 2Kg the wear is minimal in micron at sliding distance of 500, 750, and 1000 compared to 4Kg and 6 Kg load at 4Kg load maximum wear is seen at sliding distance of 750, similarly for 6kg load maximum wear is seen at sliding distance of 1000 compared to 2kg and 4kg and for weight percentage of 2wt%, 4wt% and 6wt% in the loading condition of 6Kg removal of material with varying percentage is seen much difference as the wear removal is in the order of 10^{-7}. Adhesive wear takes place at minimum loading condition. But abrasive wear takes place at the higher loading condition and wear increase by means of increase in applied load. It is found that the wear rate was reliant on the hardness of the material, but it is not always related to hardness. Toughness and equal circulation of reinforcement in Al matrix are the dependent factors for wear.

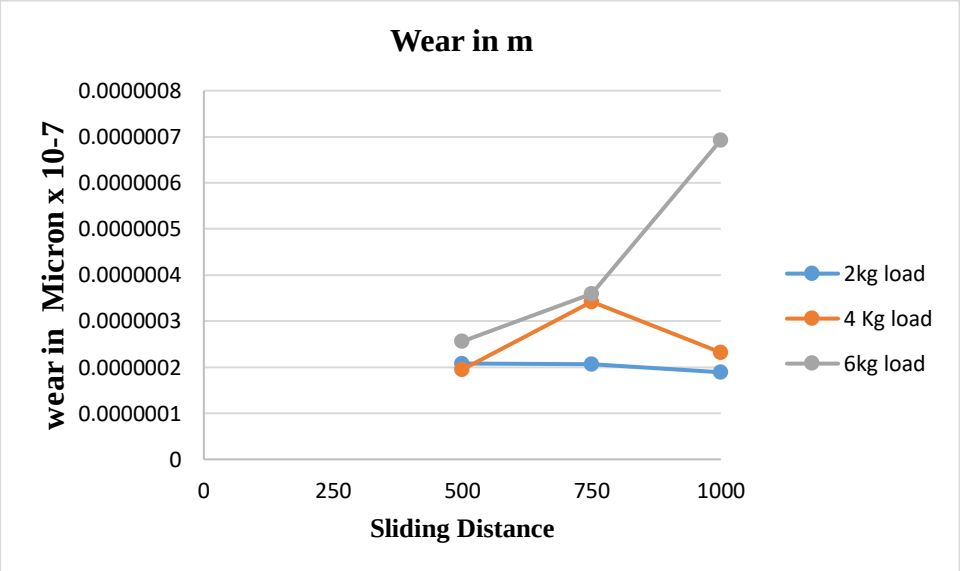

Figure 7.1 Wear in m with 2, 4 and 6 kg load with sliding distance 500,750 and 1000

Power System Technology
ISSN:1000-3673
Received: 16-01-2024 Revised: 12-02-2024 Accepted: 07-03-2024

Table 7.1 shows % composition, load in Kg, sliding Distance and wear in meter.

Sl	% Composition	Load in Kg	Sliding Distance	Wear in m
1	2	2	500	2.08E-07
2	2	6	500	2.56E-07
3	2	4	500	1.95E-07
4	4	4	750	3.42E-07
5	4	2	750	2.07E-07
6	4	6	750	3.59E-07
7	6	6	1000	6.93E-07
8	6	4	1000	2.32E-07
9	6	2	1000	1.89E-07

8. Vickers Hardness

The Vickers Hardness test (ISO 6507) is used to characterize hardness of various solid materials (metals, ceramics, etc.).The Vickers Hardness Test uses a diamond indenter in the appearance of a right pyramid with a square base and an angle of 136 degress between opposite faces. The indenter is subjected to a load of 1 to 100 kgf. The full load is applied for 10 to 15 seconds. The two diagonals left in the surface of the material are measured using a microscope and their average is taken.

The Vickers hardness (HV) is calculated by the formula, $HV = 0.1891 * F/d^2$, Where d is the middling of the two diagonals of imprints and F is the load applied

Hardness in GPA is calculated as follows, $H= (0.1891*9.8/1000)* F/d^2$.

The yield stress can be approximated from the hardness using the formula $\sigma_u = HV/0.3$

Table 8.1 Hardness value in GPa

HAMC	0%	2%	4%	6%
Hardness value	46.32	57.19	74.23	91.90
Hardness GPa	0.45	0.56	0.72	0.90
Yield stress N/mm^2	154.43	190.6	247.4	306.3

Power System Technology
ISSN:1000-3673
Received: 16-01-2024 Revised: 12-02-2024 Accepted: 07-03-2024

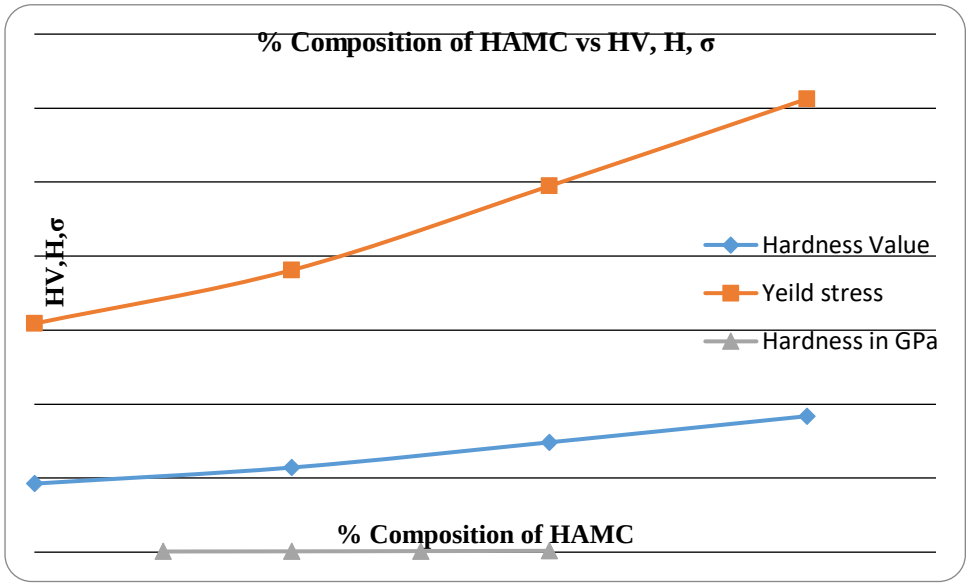

Figure 8.1 Weight % composition of HAMC vs. HV, H, and yield stress

9. X-ray Diffraction-

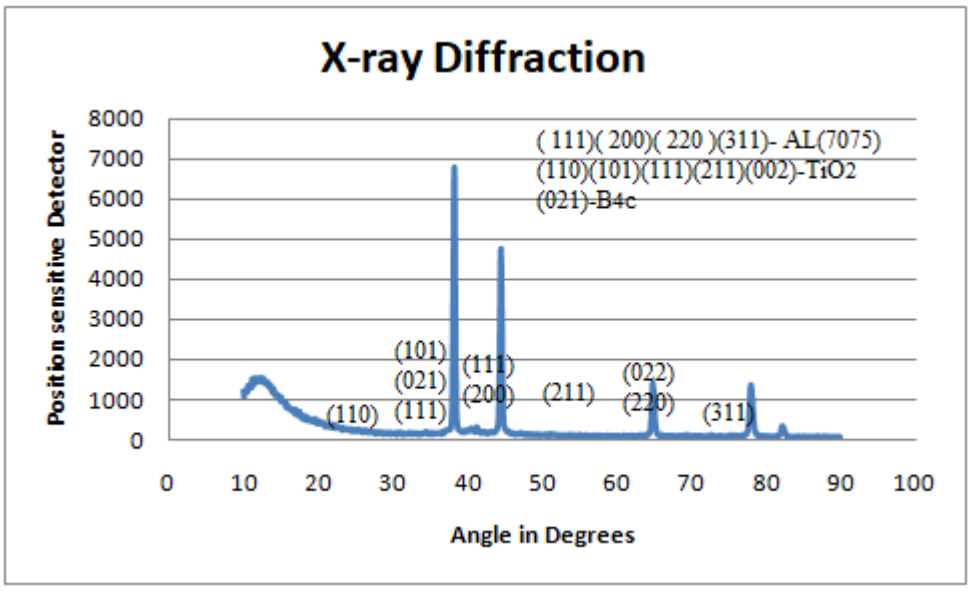

Figure 9.1 X ray diffraction of HAMC

Figure 9.1. Shows the elemental maps of aluminium matrix reinforced with 2 wt. % of B_4C particles and 1 wt% of tio_2 as of the elemental maps of the composite it is evident that the main elements present in the composite are Al (largest amount) and B (second largest amount)

Power System Technology
ISSN:1000-3673
Received: 16-01-2024 Revised: 12-02-2024 Accepted: 07-03-2024

whereas Mg, Ti, Cu and Zn which be constituents of base metal Al7075 are also present in small amount.

The peak at 2q value of 37.58 corresponds to B4C (JCPDS 33–0225) with miller indices of (021). The peaks corresponding to the aluminium matrix at 38.48, 44.74, 65.10, 78.23 with miller indices of (111), (200), (220) and (311), respectively are clearly evident. The position of 2θ at 27.42°, 36.08°, 41.25°, 54.33° and 63.44° corresponds to tio_2 miller indices of (110), (101), (111), (211) and (002) plane, respectively[6-14-13-10].

10. EDAX-

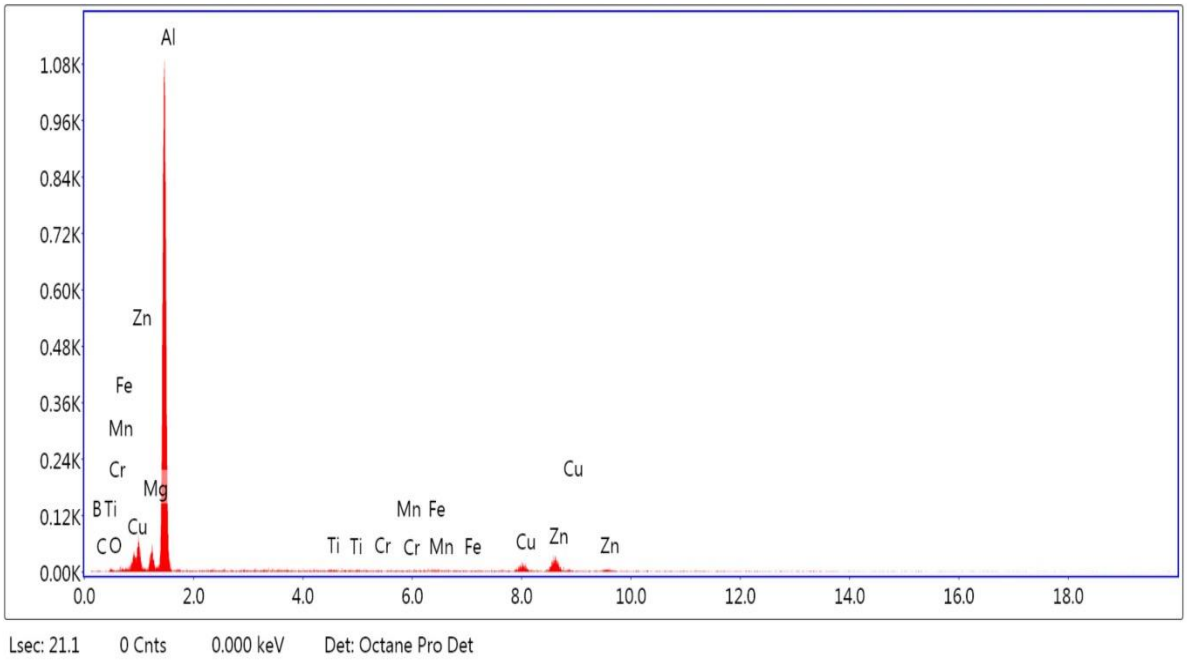

Figure.10.1 shows XRD results and the details about the elements present in the manufactured composites.

Table 10.1 Elements present in the manufactured composites with weight% and Atomic%

Element	Weight %	Atomic %
B K	15.99	32.83
C K	2.85	5.26
O K	1.46	2.03
MgK	3.06	2.79

Power System Technology
ISSN:1000-3673
Received: 16-01-2024 Revised: 12-02-2024 Accepted: 07-03-2024

AlK	64.05	52.67
TiK	0.31	0.14
CrK	0.28	0.12
MnK	0.23	0.09
FeK	0.54	0.22
CuK	3.76	1.31
ZnK	7.47	2.53

Table 10.1 shows the elements there in the Al7075+ 2% B_4C and 1 wt% of tio_2 reinforced composites among their weight percentage and atomic percentage in composite. The elemental maps verify that the manufactured composite is reinforced with B_4C and Tio_2 particles. The energy dispersion spectrum (EDS) analysis was carried out on the B4C particles and Al matrix, Figure10. The energy dispersion spectrum taken from B4C particle indicates the presence of boron, carbon, oxygen, magnesium, silicon and aluminium [10]

11. Scanning Electron Microscope

0% B4C

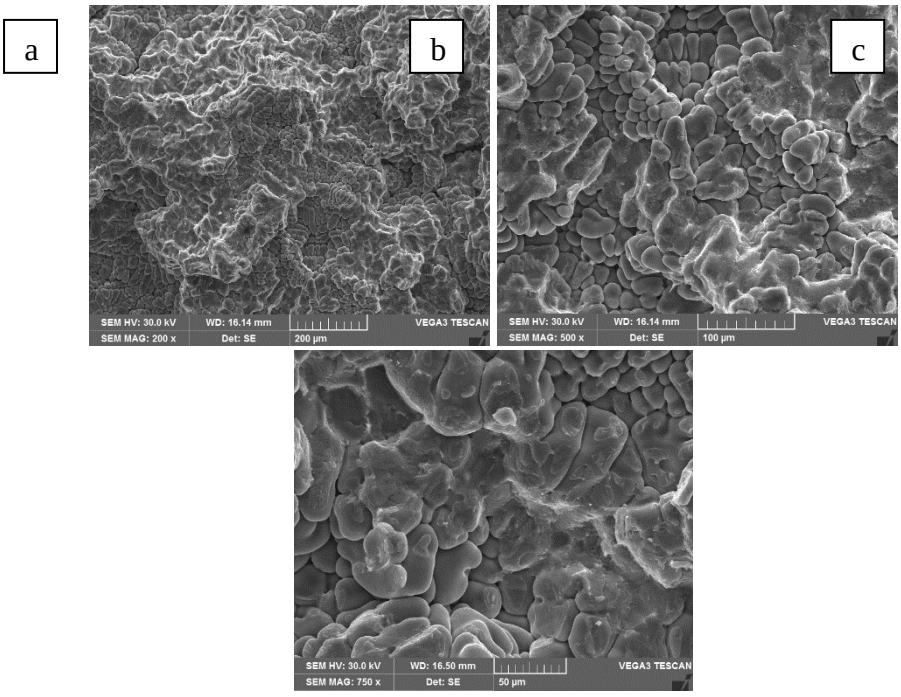

Figure11.1 a, b, c SEM images at 200micrometer, 100micrometer and 50micrometer

Power System Technology
ISSN:1000-3673

Received: 16-01-2024 Revised: 12-02-2024 Accepted: 07-03-2024

2% B4C

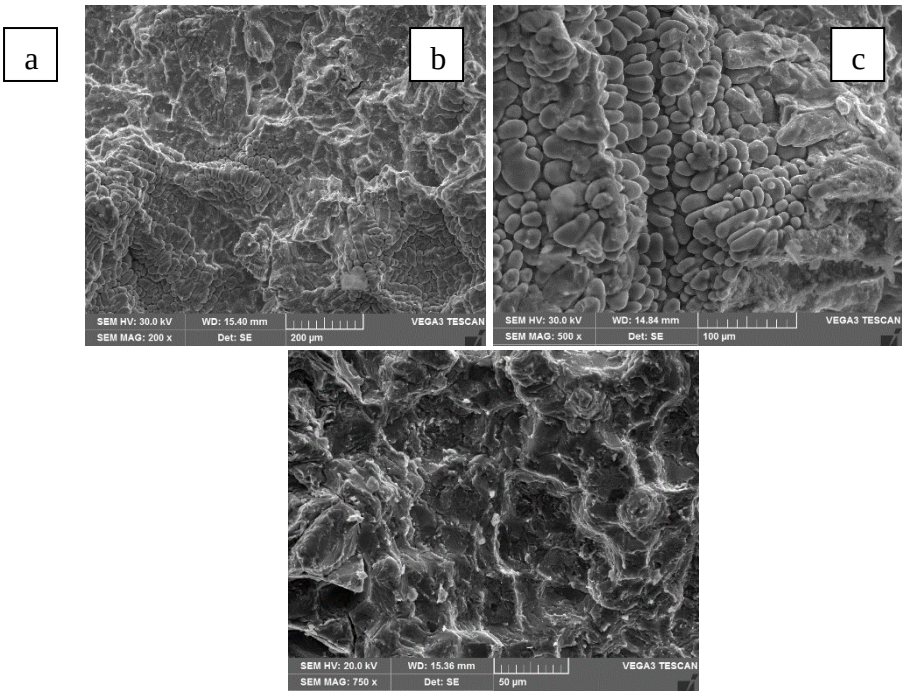

Figure11.2 a, b, c SEM images at 200micrometer, 100micrometer and 50micrometer

4% B4C

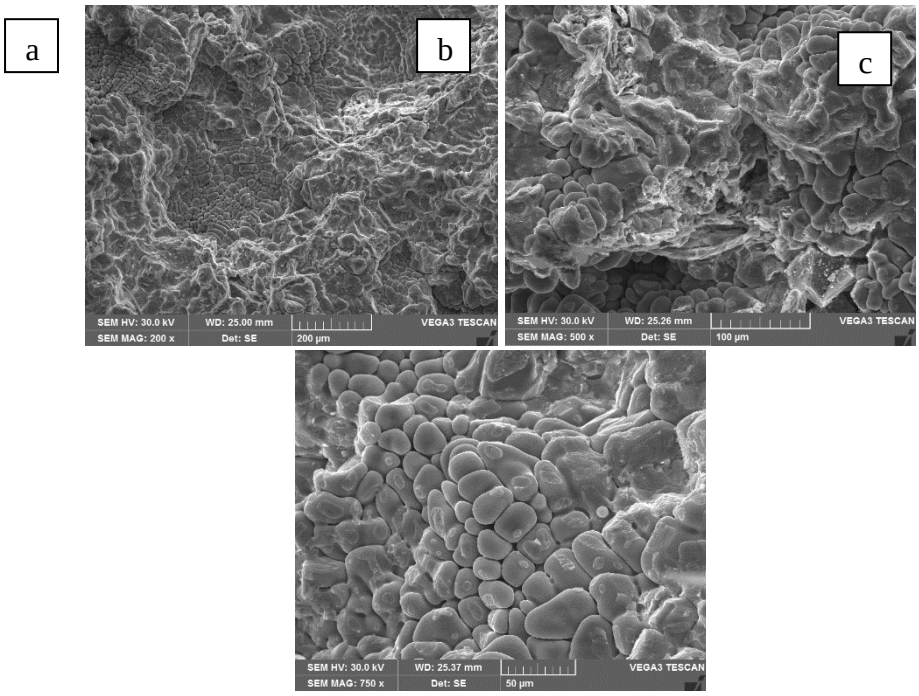

Figure11.3 a, b, c SEM images at 200micrometer, 100micrometer and 50micrometer

Power System Technology
ISSN:1000-3673
Received: 16-01-2024 Revised: 12-02-2024 Accepted: 07-03-2024

6% B4C

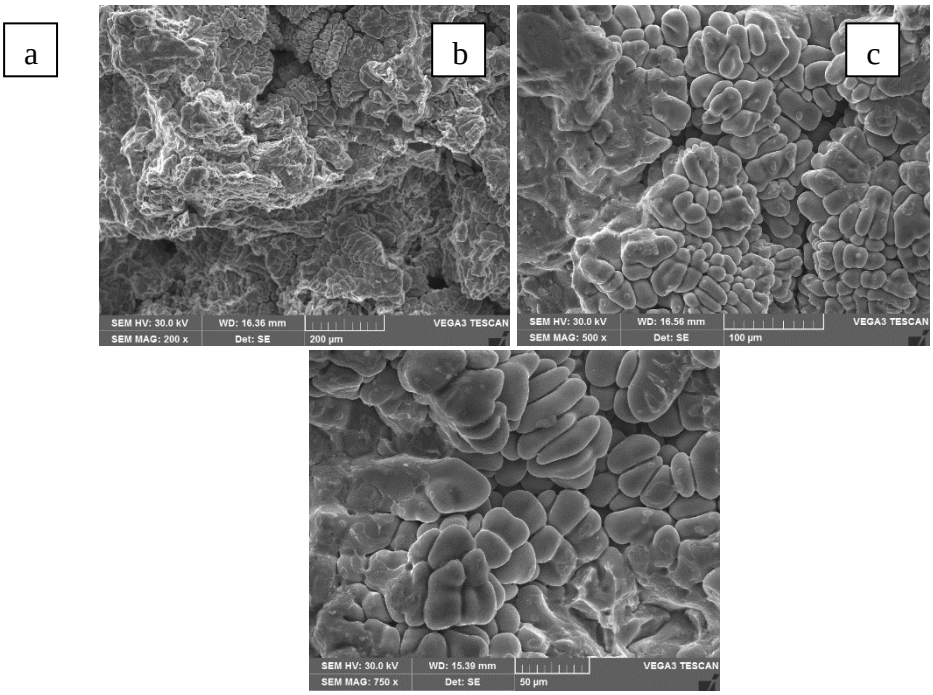

Figure11.4 a, b, c SEM images at 200micrometer, 100micrometer and 50micrometer

The first requirement for a composite material to show its superior performance is the homogeneous sharing of the reinforcing phases. The agglomeration of the reinforcement particles deteriorate the mechanical properties of the composite, are dependent upon the spatial distribution of reinforcing phase and particle morphology [4-5]. The magnitude and morphology of the particulates constitute the matrix and reinforcement also influence the mechanical and physical properties of the composite.SEM picture of Insitu (Al7075 + B_4C+ Tio_2) based aluminium metal matrix composite images shown at different focus of 200micro meter, 100micro meter and 50 micro meter with diiffrent weight percentage of 0%wt, 2% wt, 4%wt and 6%wt reinforcement, in each of the images three distinct micro structural arrangements are observed corresponding to the different phases peritectic (α + Al_3Ti) and binary phases solid (TiB_2), (α + Al_2O_3) and (α Ti) formed by solid-state reaction and inter-diffusion within the elements. With different focus in the images of 0wt% of a, b and c in the image (a) addition of titanium oxide is seen like white flakes and images (b) and (c) bonding with no significant agglomeration and clustering of particles were observed. With the adding up of B_4C in 2wt% with different focuses image (a) and image (b) the presence of B_4C has seen like black flakes in the image (c) and weight 4wt% and 6wt% percentage of the hybrid aluminium metal matrix composite no agglomeration and not much clustering of particles along with the void were less noticed No large agglomerations of Al_3Ti particulates and porosity were noticed [18]. But composites with larger Matrix (TiB_2 +Tic) Particle Clustering

Power System Technology
ISSN:1000-3673
Received: 16-01-2024 Revised: 12-02-2024 Accepted: 07-03-2024

reinforcement particles tend to cluster in the matrix region. Particle clustering occurs because of a high surface area of particle and the action of the Van der Waals attraction force of bulky particle [26]. Wide particle free zones and large interparticle spacing in the matrix were observed for the lower volume fraction of B_4C particles, particle free zone decreases with an increase in amount content of the reinforcement and the distribution of B4C particles in the AL matrix becomes relatively homogeneous and discrete. The experimental fact that B4C, TiO_2 particulates with small particle size, homogeneously distributed around the aluminium matrix region. The pattern of the particle distribution in the composite microstructure is largely determined by the solidification process. The solidification of the particle reinforced metal matrix composites is most powerfully influenced by the cooling rate: The higher the cooling rate the more uniform is the particle distribution [1-8]. An increase in the cooling rate minimizes the particle segregation due to particle rejection at the solidification front which results in much more homogeneous distribution of the particle. At slow cooling rates, particles are rejected and pushed ahead of the solidification front resulting in the clustering of particles.

12. Conclusion;

Insitu (Al7075-B_4C-TiO2) mongrel essence matrix mixes composites were productively fabricated with equal proportion (2 wt. %, 4wt. %, 6 wt. %, 8 wt. %) of mounts. Viscosity computation, Mechanical Parcels, Compression, Impact and Tribological parcels, Vickers hardness, wear rate and x-ray diffraction, EDAX and SEM of the worn surface, cold blooded essence matrix mixes were considered. The perfected commentaries of present experimental work are as follows:

1. Mechanical parcels of Insitu (Al7075-B_4C-TiO2) mongrel increase with increase weight chance of underpinning. Maximum axial force of tensile instance, seen (17.15 kN,18.26 kN,18.72 kN and 20.94 kN), Compresive cargo bearing capacity of the samples is (237.3kN, 243.9kN, 263.15kN and 277.22kN)and Imapct energy observed is 2.214,2.328,2.457 and 2.661 incraeses with varying adding in underpinning with 0%wt, 2% wt, 4%wt and 6%wt.
2. Vickers hardness of Insitu (Al7075-B_4C-TiO2) compound material increases with increase in chance of mounts. Maximum hardness of 0.9Gpa is seen at 6wt% of mongrel aluminium essence matrix mixes.
3. Wear rate Insitu (Al7075-B_4C-TiO2) mongrel mixes decreases with difference of underpinning from varying cargo 2Kg,4Kg and 6Kg the cause is slicking parcels of titanium oxide patches which favours for the increase within wear and tear resistance.
4. Scanning Electron Microscopy is used for worn face analysis; it is bring into being that lower deep groves, lower debris and lower rough shells in advance chance of underpinning Insitu (Al7075-B_4C-TiO2) fabrication of mongrel aluminium essence matrix mixes.

Power System Technology
ISSN:1000-3673

Received: 16-01-2024 Revised: 12-02-2024 Accepted: 07-03-2024

References:

1. B M, K., M C, G., Sharma, S., Hiremath, P., Shettar, M., & Shetty, N. (2020). Coated and uncoated reinforcements metal matrix composites characteristics and applications – A critical review. Cogent Engineering, doi:10.1080/23311916.2020.1856758
2. Ibrahim, I. A., Mohamed, F. A., & Lavernia, E. J. (1991). Particulate reinforced metal matrix composites ? a review. Journal of Materials Science, 26(5), 1137–1156. doi: 10.1007/bf00544448
3. Chawla, N., & Shen, Y.-L. (2001). Mechanical Behaviour of Particle Reinforced Metal Matrix Composites. Advanced Engineering Materials. doi:10.1002/1527-2648(200106)
4. Mohanavel, V., Ravichandran, M., & Suresh Kumar, S. (2019). Tribological and mechanical properties of Zirconium Di-boride (ZrB2) particles reinforced aluminium matrix composites. Materials Today: Proceedings. doi:10.1016/j.matpr.2019.07.603
5. Khan, M., Zulfaqar, M., Ali, F., & Subhani, T. (2017). Hybrid aluminium matrix composites containing boron carbide and quasicrystals: manufacturing and characterisation. Materials Science and Technology, 33(16), 1955–1963. doi:10.1080/02670836.2017.1342017
6. Domnich, V., Reynaud, S., Haber, R. A., & Chhowalla, M. (2011). Boron Carbide: Structure, Properties, and Stability under Stress. Journal of the American Ceramic Society, 94(11), 3605–3628. doi:10.1111/j.1551-2916.2011.04865.
7. David Raja Selvam, J., Dinaharan, I., Rai, R. S., & Mashinini, P. M. (2019). Role of zirconium diboride particles on microstructure and wear behaviour of AA7075 in situ aluminium matrix composites at elevated temperature. Tribology - Materials, Surfaces & Interfaces, 13(4), 230–238. doi.org/10.1080/17515831
8. Kumar, N., Gautam, G., Gautam, R. K., Mohan, A., & Mohan, S. (2015). Synthesis and Characterization of TiB2 Reinforced Aluminium Matrix Composites: A Review. Journal of the Institution of Engineers (India): Series D, 97(2), 233–253. doi: 10.1007/s40033-015-0091-7
9. Chauhan, Ankur; Schaefer, Mark C.; Haber, Richard A.; Hemker, Kevin J. (2019). Experimental observations of amorphization in stoichiometric and boron-rich boron carbide. Acta Materialia, (), S1359645419306421–. doi:10.1016/j.actamat.2019.09.052
10. Chawla, N., & Shen, Y.-L. (2001). Mechanical Behaviour of Particle Reinforced Metal Matrix Composites. Advanced Engineering Materials. doi:10.1002/1527-2648(200106)
11. Qi, W. J., Song, R. G., Zhang, Y., Wang, C., Qi, X., & Li, H. (2015). Study on mechanical properties and hydrogen embrittlement susceptibility of 7075 aluminium alloy. Corrosion Engineering, Science and Technology, 50(6), 480–486. doi: 10.1179/1743278215
12. Alizadeh, A., Taheri-Nassaj, E., Ehsani, N., & Baharvandi, H. R. (2006). Production of boron carbide powder by carbothermic reduction from boron oxide and petroleum coke or

Power System Technology
ISSN:1000-3673
Received: 16-01-2024 Revised: 12-02-2024 Accepted: 07-03-2024

carbon active. Advances in Applied Ceramics, 105(6), 291–296. doi: 10.1179/174367606x146685

13. Yu, J., Zhao, Q., Huang, S., Zhao, Y., Zhou, Y., Lu, J.Zhang, Y. (2021). Effect of sintering temperature on microstructure and properties of graphene nanoplatelets reinforced TC21 composites prepared by spark plasma sintering. Journal of Alloys and Compounds, 879, 160346. doi:10.1016/j.jallcom.2021.16034
14. Kerti, I., & Toptan, F. (2008). Microstructural variations in cast B4C-reinforced aluminium matrix composites (AMCs). Materials Letters, 62(8-9), 1215–1218. doi:10.1016/j.matlet.2007.08.015
15. Kokulnathan, T., Ashok Kumar, E., & Wang, T.-J. (2020). Design and In Situ Synthesis of Titanium Carbide/Boron Nitride Nanocomposite: Investigation of Electro catalytic activity for the sulfadiazine sensor.ACS sustainable chemistry and Engineering doi:10.1021/acssuschemeng.0c03281
16. Jung, J., & Kang, S. (2004). Advances in Manufacturing Boron Carbide-Aluminum Composites. Journal of the American Ceramic Society, 87(1), 47–54. doi:10.1111/j.1551-2916.2004.00047.
17. Jiang, L., Yang, H., Yee, J. K., Mo, X., Topping, T., Lavernia, E. J., & Schoenung, J. M. (2016). Toughening of aluminum matrix nanocomposites via spatial arrays of boron carbide spherical nanoparticles, Acta Matetrialia, 103,128-140.doi 10.1016/j.actamat.2015.09.057.
18. Arévalo, C., Montealegre-Meléndez, I., Ariza, E., Kitzmantel, M., Rubio-Escudero, C., & Neubauer, E. (2016). Influence of Sintering Temperature on the Microstructure and Mechanical Properties of In Situ Reinforced Titanium Composites by Inductive Hot Pressing. Materials, 9(11), 919. doi: 10.3390/ma9110919
19. Monteverde, F., Bellosi, A., & Guicciardi, S. (2002). Processing and properties of zirconium diboride-based composites. Journal of the European Ceramic Society, 22(3), 279–288. doi: 10.1016/s0955-2219(01)00284-9
20. Sahu, J. K., Sahoo, C. K., & Masanta, M. (2015). In-Situ TiB2–TiC–Al2O3 Composite Coating on Aluminum by Laser Surface Modification. Materials and Manufacturing Processes, 30(6), 736 742. doi:10.1080/10426914.2014.984225
21. P. Gnaneswaran, V. Hariharan, Samson Jerold Samuel Chelladurai, G. Rajeshkumar, S. Gnanasekaran, S. Sivananthan, Baru Debtera, "Investigation on Mechanical and Wear Behaviors of LM6 Aluminium Alloy-Based Hybrid Metal Matrix Composites Using Stir Casting Process", Advances in Materials Science and Engineering, vol. 2022, Article ID 4116843, 10 pages, 2022. https://doi.org/10.1155/2022/4116843
22. Zhang, G.-J., & Ohji, T. (2004). In Situ Reaction Synthesis of Silicon Carbide-Boron Nitride Composites. Journal of the American Ceramic Society, 84(7), 1475–1479. doi:10.1111/j.1151-2916.2001.tb00863.x

Power System Technology
ISSN:1000-3673
Received: 16-01-2024 Revised: 12-02-2024 Accepted: 07-03-2024

23. Singh, G., & Goyal, S. (2016). Dry sliding wear behaviour of AA6082-T6/SiC/B4C hybrid metal matrix composites using response surface methodology. Proceedings of the Institution of Mechanical Engineers, Part L: Journal of Materials: Design and Applications, 146442071665711. doi:10.1177/1464420716657114
24. Hassan, S. F., & Gupta, M. (2003). Development of high strength magnesium copper based hybrid composites with enhanced tensile properties. Materials Science and Technology, 19(2), 253–259. doi: 10.1179/026708303225009346
25. Lee, M. (2004). Fabrication of Ni–Nb–Ta metallic glass reinforced Al-based alloy matrix composites by infiltration casting process. Scripta Materialia, 50(11), 1367–1371. doi:10.1016/j.scriptamat.2004.02
26. Madhavan, S., Kamaraj, M., & Vijayaraghavan, L. (2016). Cold metal transfer welding of aluminium to magnesium: microstructure and mechanical properties. Science and Technology of Welding and Joining, 21(4), 310–316. doi:10.1080/13621718.2015.1108070
27. Gao, Y.-Y., Dong, B.-X., Qiu, F., Geng, R., Wang, L., Zhao, Q.-L., & Jiang, Q.-C. (2018). The superior elevated-temperature mechanical properties of Al-Cu-Mg-Si composites reinforced with in situ hybrid-sized TiC x -TiB 2 particles. Materials Science and Engineering: A, 728, 157164. doi:10.1016/j.msea.2018.05.024
28. Ho, K. ., Gupta, M., & Srivatsan, T.(2004). The mechanical behavior of magnesium alloy AZ91 reinforced with fine copper particulates. Materials Science and Engineering: A, 369(1-2), 302 308. doi:10.1016/j.msea.2003.11.011
29. Sonber, J. K., Murthy, T. S. R. C., Subramanian, C., Fotedar, R. K., Hubli, R. C., & Suri, A. K. (2013). Synthesis, Densification and Characterization of Boron Carbide. Transactions of the Indian Ceramic Society, 72(2), 100–107. doi:10.1080/0371750x.2013.817755
30. Peter P., I., M., O., & Adekunle A., A. (2020). A review of ceramic/bio-based hybrid reinforced aluminium matrix composites Cogent engineering doi:10.1080/23311916.2020.1727167
31. Liu, J., & Ownby, P. D. (1991). Boron Carbide Reinforced Alumina Composites. Journal of the American Ceramic Society, 74(3), 674–677. doi:10.1111/j.1151-2916.1991.tb04081.x
32. Raj, R., & Thakur, D. G. (2018). Influence of boron carbide content on the microstructure, tensile strength and fracture behavior of boron carbide reinforced aluminum metal matrix composites. Material wissenschaft and Werkstofftechnik, 49(9), 1068–1080. doi:10.1002/mawe.201700086
33. Arévalo, C., Montealegre-Meléndez, I., Ariza, E., Kitzmantel, M., Rubio-Escudero, C., & Neubauer, E. (2016). Influence of Sintering Temperature on the Microstructure and

Power System Technology
ISSN:1000-3673

Received: 16-01-2024 Revised: 12-02-2024 Accepted: 07-03-2024

Mechanical Properties of In Situ Reinforced Titanium Composites by Inductive Hot Pressing. Materials, 9(11), 919. doi: 10.3390/ma9110919

34. Vineeth Kumar, K., & Jayahari, L. (2018). Study of Mechanical Properties and Wear Behaviour of Aluminium 6063 Matrix Composites Reinforced With Steel Machining Chips. Materials Today: Proceedings, 5(9), 20285–20291. doi:10.1016/j.matpr.2018.06.400
35. Sahu, M. K., & Sahu, R. K. (2020). Experimental Investigation, Modeling, and Optimization of Wear Parameters of B4C and Fly-Ash Reinforced Aluminum Hybrid Composite. Frontiers in Physics, 8. doi:10.3389/fphy.2020.00219

Appendix-1

Calculation of density of Composite material

SYMBOLS

ρ Density, (g/cm^3)

A_w Atomic weight, (g/mol)

V_c Volume of each unit cell, (cm^3)

n or Z number of atoms per unit cell

N_A Avogadro's number = 6.023*10^{23} (atoms /mol)

a Edge length, (cm)

r radius of an atom, (cm)

1. Density of Aluminium 7075.

w.k.t Density is given by $\boldsymbol{\rho = \frac{n*A_w}{V_C*N_A}}$

Data: n = 4 (since Al 7075 has FCC lattice structure).

A_w = 26.9815 g/mol.

N_A = 6.023*10^{23} (atoms /mol).

$V_c = a^3$, where $a = \frac{4r}{\sqrt{2}}$, a = 4.0446*10^{-8} cm.

$a = \frac{4*0.143*10^{-7}}{\sqrt{2}}$

a = 4.0446*10^{-8} cm

Power System Technology
ISSN:1000-3673
Received: 16-01-2024 Revised: 12-02-2024 Accepted: 07-03-2024

r = 0.143*10^{-7} cm.

Hence density is $\rho = \frac{4*26.9815}{(4.0446*10^{-8})^3*6.023*10^{23}}$ = 2.7083 g/cm^3

Therefore, density is 2.7083 g/cm^3.

2. **Density of Titanium**

w.k.t Density is given by $\boldsymbol{\rho = \frac{n*A_w}{V_C*N_A}}$

Data: n = 6 (since Titanium has HCP lattice structure).

A_w = 47.867 g/mol.

N_A = 6.023*10^{23} (atoms /mol).

$V_c = 24 * \sqrt{2} * r^3 = 1.07814 * 10^{-22}$ cm^3.

r = 0.147*10^{-7} cm.

Hence density is $\rho = \frac{6*47.867}{1.07814*10^{-22}*6.023*10^{23}}$ = 4.4228 g/cm^3.

3. **Density of Boron Carbide (B_4C)**

w.k.t Density is given by $\boldsymbol{\rho = \frac{n*A_w}{V_C*N_A}}$

Data: n = 4 (since Boron carbide has Rhombohedral lattice structure).

A_w = 55.255 g/mol.

N_A = 6.023*10^{23} (atoms /mol).

$V_c = (2 * r)^3$ cm^3.

r = 2.6375*10^{-8}

Hence density is $\rho = \frac{6*55.255}{(2*2.6375*10^{-8})^3*6.023*10^{23}}$ = 2.5 g/cm^3.

Power System Technology
ISSN:1000-3673
Received: 16-01-2024 Revised: 12-02-2024 Accepted: 07-03-2024

4. Density of composite material

Steps followed are as follows: -

- Find the densities of all the compounds (or elements) in the mixture.

Density of Al 7075 = 2.7083 g/cm^3
Density of TiO_2 = 4.4228 g/cm^3
Density of B_4C = 2.5 g/cm^3

- Convert each element or compound's percentile contribution to the mixture to a decimal number (a number between 0 and 1) by dividing by 100.

Al 7075 = 2.7083* 0.97 = 2.6271 g/cm^3
TiO_2 = 4.4228*0.01 = 0.044228 g/cm^3
B_4C (0%) = 2.5 *0 = 0 g/cm^3
B_4C (2%) = 2.5 *0.02 = 0.05 g/cm^3
B_4C (4%) = 2.5 *0.04 = 0.1 g/cm^3
B_4C (6%) = 2.5 *0.06 = 0.15 g/cm^3

- Add together the products from step 2.

Therefore,

1) Density of composite (B_4C 0%) = 2.6271 + 0.044228 + 0 = 2.6713 g/cm^3

2) Density of composite (B_4C 2%) = 2.6271 + 0.044228 + 0.05 = 2.7213 g/cm^3

3) Density of composite (B_4C 4%) = 2.6271 + 0.044228 + 0.1 = 2.7713 g/cm^3

4) Density of composite (B_4C 6%) = 2.6271 + 0.044228 + 0.15 = 2.8213 g/cm^3

Experimental Density Calculation

We know that density is given by $\boldsymbol{\rho = \frac{mass}{Volume}}$

As the specimen are of cylindrical shape volume is given by $\boldsymbol{V = \pi r^2 h}$ **cm^3**

Power System Technology
ISSN:1000-3673

Received: 16-01-2024 Revised: 12-02-2024 Accepted: 07-03-2024

Sl.No	Composition	Mass in g	Radius in cm	Height in cm	Volume in cm^3	Density in g/cm^3
1)	6%	7	0.5625	2.93	2.8945	2.4183
2)	4%	8	0.6	2.64	3.293	2.6793